Antitumoral and Mechanistic Studies of Ianthelline Isolated from the Arctic Sponge *Stryphnus fortis*

KINE Ø. HANSSEN[1], JEANETTE H. ANDERSEN[2], TRINE STIBERG[2], RICHARD A. ENGH[3], JOHAN SVENSON[4], ANNE-MARIE GENEVIÈRE[5] and ESPEN HANSEN[2]

[1]*Centre for Research-based Innovation on Marine Bioactivities and Drug Discovery (MabCent),*
[2]*Marbio,* [3]*The Norwegian Structural Biology Centre (NorStruct) and*
[4]*Department of Chemistry, University of Tromsø, Breivika, Tromsø, Norway;*
[5]*Université Paris 06, Laboratoire Arago, Banyuls-sur-Mer, France*

Abstract. *Background: Ianthelline was isolated from the Arctic sponge Stryphnus fortis. The structure of the compound has been previously described. However, only limited bioactivity data are available and little has been reported about the cytotoxic potential of ianthelline since its discovery. In addition, no study has so far aimed at identifying which cellular mechanisms are affected by ianthelline to generate cytotoxicity. Materials and Methods: The cytotoxicity of ianthelline was tested against one non-malignant and ten malignant cell lines. The effects of ianthelline on key cell division events were studied in sea urchin embryos. Tyrosine kinase ABL (ABL), cAMP-dependent protein kinase A (PKA), protein-tyrosine phosphatase 1B (PTP1B), and a panel of 131 kinases were further tested for sensitivity to ianthelline. Results: Ianthelline inhibits cellular growth in a dose- and time-dependent manner. Disturbed mitotic spindle formation was found in sea urchin embryos exposed to ianthelline. In addition, pronuclear migration and cytokinesis were severely inhibited. No effect on DNA synthesis was detectable. Ianthelline did not significantly inhibit ABL, but did provoke weak dose-dependent inhibition of PKA and PTP1B. It strongly inhibited the activity of 1 out of 131 tested kinases (to residual activity <10 %), with a Gini co-efficient of 0.22 for the degree of selectivity of kinase inhibition. Conclusion: These results demonstrate that ianthelline is a cytotoxic marine compound, which exerts its antiproliferative effects by several mechanisms that include inhibition of mitotic spindle formation and inhibition of protein kinase activity.*

Correspondence to: Kine Ø. Hanssen, MabCent, University of Tromsø, Breivika, Tromsø, Norway. Tel: +47 77649272, e-mail: kine.o.hanssen@uit.no

Key Words: Stryphnus fortis, ianthelline, marine natural product, cell viability, *Paracentrotus lividus* embryo, microtubule organisation, kinase inhibition.

Natural products play important roles in modern medicine; 63% of all small-molecule drugs introduced to the market between 1981 and 2008 were natural products or by-products (1). For anticancer drugs, the corresponding figure is even higher, 79.8%, with several recent ones originating from marine organisms. So far, natural products of marine origin have resulted in seven Food and Drug Administration-approved drugs and several compounds in pre-clinical and clinical trials (2). The anticancer agent brentuximab vedotin (Adcetris®) is an antibody-drug conjugate and is the most recently approved marine natural product derivative.

The success of natural products in modern drug discovery has been attributed to the high degree of chemical diversity, in contrast to screening libraries generated by combinatorial synthesis (3). The higher architectural complexity of natural products is reflected by their higher molecular weight, higher number of chiral centres and rings, as well as a lower number of rotatable bonds compared to compounds, originating from combinatorial synthesis (3). Secondary metabolites are natural products not essential for the growth and development of the producing organism (4). While it was previously presumed that they served no particular purpose for the producing organism, it is increasingly accepted that their biosynthesis increases the chance of species survival by acting in several ways, including as parasite and pathogen repellents (5). Throughout evolution, many secondary metabolites have co-evolved with targets in predators and parasites, and are in this way optimised for macromolecular interaction (6). Taken together, these characteristics make secondary metabolites first-class candidates in the search for novel compounds with beneficial drug-like properties.

Out of all marine species, bioactive compounds have been detected especially frequently in sponges (2). Sponges are sessile aquatic organisms belonging to the phylum Porifera. More than 10,000 species are known, most of them of marine origin, and they are found all over the world (7, 8). Sponges rely not only on mechanistic protection *via* spicules, but also

on a diverse chemical arsenal of secondary metabolites. As a result, a range of different bioactive natural products has been isolated from marine sponges, including compounds with anticancer (9, 10), antibacterial (11), antiviral (12), anti-inflammatory (13), and immunostimulatory (14) effects.

In this work, the secondary metabolite ianthelline (Figure 1) was isolated from the Arctic marine sponge *Stryphnus fortis* (Figure 2). Ianthelline was identified as the main compound in fractions of the organic extract from *S. fortis,* exhibiting anticancer activity in the MabCent screening program. It was isolated from the Bahamian sponge *Ianthella ardis* and was characterized by Litaudon and Guyot in 1986 (15). In 2010, it was synthesized by Shearman *et al.* (16). Despite its chemical structure being known for years, only limited data are available on its antiproliferative properties. In the current study, the cytotoxic potential of the compound against both malignant and non-malignant cell lines is described. In addition, the cytotoxic mode of action is investigated by employing *Paracentrotus lividus* embryos to examine the effect of ianthelline on cell-cycle progression, DNA synthesis, microtubule organisation, and cytokinesis. Furthermore, the ability of ianthelline to inhibit enzyme activity was investigated. Tyrosine kinase ABL (ABL), cAMP-dependent protein kinase A (PKA) and protein-tyrosine phosphatase 1B (PTP1B) were tested for sensitivity against ianthelline. To characterize the kinase inhibition selectivity profile of ianthelline, the compound was tested against a panel of 131 kinases. All enzymes tested are especially interesting because of their relevance to anticancer drug discovery. PTP1B has been found to be a positive factor in cancer phenotypes (17), and protein kinases are the proteins most frequently mutated in malignant tumours (18).

Materials and Methods

Sample collection. S. fortis specimens were collected with an Agassiz dredge trawl at a depth of 333 m, northwest of Spitsbergen (79˚33'N, 8˚53'E) in September 2007. The biomass sample was stored at -23˚C until further use and a reference specimen was deposited as a sub-sample at the Norwegian National Marine Biobank (Marbank), University of Tromsø, Norway.

Extraction. Freeze-dried *S. fortis* was ground and extracted twice with ultra-pure water (Milli-Q; Millipore, Billerica, MA, USA) (24 h and 30 min) at 5˚C in the dark. After centrifugation and supernatant removal, the remaining sediment was freeze-dried, ground, and extracted twice with a 1:1 (vol:vol) mixture of dichloromethane (Merck, Darmstadt, Germany) and methanol (MeOH) (Sigma-Aldrich, Steinheim, Germany) (24 h and 30 min) at 5 ˚C in the dark. The mixture was vacuum-filtered through a Whatman Ø 125 mm no. 3 filter (Little Chalfont, UK) and the resulting supernatant was reduced to a concentrated liquid under vacuum. The extract was stored at –23˚C until further analysis.

Isolation of ianthelline. Organic extract (2 g) was dissolved in 80 ml n-hexane (Merck) and transferred to a separating funnel to which 40 ml of 90% MeOH were added for liquid-liquid partitioning purification. After mixing and phase separation, the MeOH phase was collected and the hexane phase re-extracted using 40 ml of 90% MeOH. The combined MeOH phases were reduced to 1 ml under vacuum and 2 g Dainon® HP-20SS (Supelco Analytical, Bellefonte, PA, USA) were added. The mixture was dried under vacuum in a centrifugal evaporator and applied to the top of a flash column (Biotage® SNAP, Uppsala, Sweden) packed with 6 g HP-20SS pre-equilibrated with 1:1 (vol:vol) MeOH:ultra-pure water. Fractionation was performed using a Biotage HPFC SP4 flash purification system (Uppsala, Sweden) employing increasing concentrations of MeOH in ultra-pure water and acetone (Sigma-Aldrich). All flash fractions were submitted to high-resolution mass spectrometry (HR-MS) for analysis, and fractions 8-15 were found to contain ianthelline and were combined. The fractions were concentrated under vacuum and further purified by preparative high-performance liquid chromatography (prep-HPLC). The prep-HPLC system consisted of a 600 Pump a 2996 Photodiode Array UV detector, a 3100 Mass Detector, and a 2767 sample manager (Waters, Milford, MA, USA). Waters MassLynx version 4.1 and Waters FractionLynx software were used to control the system. The mass of ianthelline was used as a fraction trigger. Aliquots of 300 µl of the concentrated fractions were injected onto a Waters XTerra RP18 HPLC column (10×300 mm, 10 µm particle size). Acetonitrile (Chromasolv; Sigma-Aldrich) and ultra-pure water, both containing 0.1% formic acid (Pro-analysis, Merck), were used as eluents. A linear gradient from 30 to 50% acetonitrile in ultra-pure water was applied at a flow rate of 6 ml/min over 10 min to elute the compound. Individual peaks from multiple injections were pooled and concentrated by evaporation.

Structure determination. The structure of ianthelline was confirmed using ultra-performance liquid chromatography (UPLC)-HR-MS analysis and nuclear magnetic resonance (NMR) spectroscopy. UPLC-HR-MS analysis was performed on an Acquity UPLC and a LCT Premier Time-of-flight MS coupled with ESI+ ionisation (Waters). The data were processed using the MassLynx software version 4.1. NMR spectra were recorded on an ianthelline sample in dimethyl sulfoxide (DMSO)-d_6 (Sigma) on a Varian 400 MHz Spectrometer (Palo Alto, CA, USA). One-dimensional ^{1}H and ^{13}C NMR experiments, two-dimensional ^{1}H-^{13}C heteronuclear single-quantum correlation (HSQC), ^{1}H-^{13}C heteronuclear multiple bond correlation (HMBC), and 1H-1H correlation spectroscopy (COSY) experiments were performed. MestreNova 5.2.4 software (Mestrelab research, Santiago de Compostela, Spain) was used to process the data.

Cell viability assay (MTS assay). The effect of ianthelline on cell viability was tested against three adherent cancer cell lines: human melanoma A2058 (American Type Culture Collection (ATCC) CRL-11147TM, Manassas, VA, USA), human breast carcinoma MCF7 (ATCC HTB-22™), and human colon carcinoma HT29 (ATCC HTB-38™); and seven suspension leukaemia cell lines: U266 (ATCC TIB-196™), Namalwa, CEM, H9, MT-4, Ramos (obtained from Dr. Michael Norcross, FDA, Bethesda, MD, USA) and SUDHL-6 (kindly provided by Dr. Mark Raffeld, National Cancer Institute, NIH, Bethesda, MD, USA). In addition, adherent, non-malignant lung fibroblasts MRC5 (ATCC CCL-171™) were used as toxicity control. Cell lines, suspended in Roswell Park Memorial Institute-1640 (RPMI) medium with 10% fetal bovine serum and 10 µg/ml gentamicin, were seeded in 96-well microtitre plates at 2,000 (adherent cell lines) or 15,000 (suspension cell lines) cells/well. The suspension cell lines were immediately exposed to different

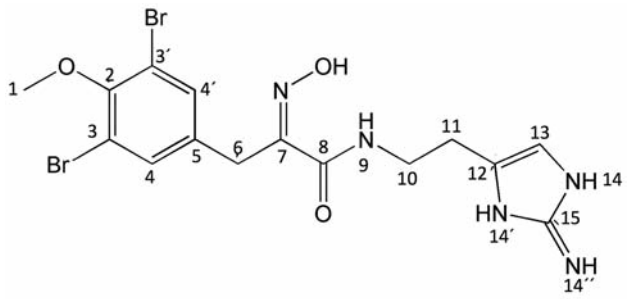

Figure 1. *Structure of ianthelline and atomic numbering of the molecule.*

concentrations of ianthelline (52-210 μM, each concentration in triplicate), and incubated for 72 h at 37˚C in a humidified atmosphere of 5% CO_2 and 95% air. The adherent cell lines were incubated for 24 h before ianthelline was added and were thereafter incubated for 72 h. Cell viability was determined by a colorimetric 3-(4,5-dimethylthiazol-2-yl)-5-(3-carboxymethoxyphenyl)-2-(4-sulfophenyl)-2H-tetrazolium (MTS) assay. At the end of the exposure time, 10 μl Cell Titer 96® Aqueous One Solution Reagent (Promega, Madison, WI, USA) was added to each well, and the plates were incubated for 1 h before absorbance was measured using a DTX 880 multimode detector (Beckman Coulter, CA, USA) at 485 nm. Cells in RPMI medium were used as negative control, and cells treated with Triton® X-100 (Sigma-Aldrich) reagent as positive control. Growth inhibition was determined by using the measured optical density (OD) and was calculated as follows: Cell survival (%)=(OD treated well – OD positive control well)/(OD negative control well–OD positive control well) ×100. The dose-dependent response to ianthelline (42-210 μM) was further investigated by monitoring the survival of A2058 cell lines after 4, 24, 48, and 72 h of exposure in 96-well microtitre plates as described above. After these incubation times, ianthelline was added to cells. Experiments were performed in triplicate. All cell lines were incubated for a total of 96 h before measuring the results, as described.

Sea urchin embryo cell-cycle progression. Sea urchins (*Paracentrotus lividus*) were collected in the Mediterranean Sea near Banyuls-sur- Mer (France), and kept in running water until use. Spawning was induced by injecting 0.2 ml of 0.2 M acetylcholine chloride solution (Sigma) into the intracoelomic cavity of the sea urchin. Resulting gametes were collected in filtered (0.22-μm membrane filter; Millipore) seawater (FSW). Collected sperm was diluted (1:10,000) in FSW. Collected eggs were washed through a 120-μm nylon filter (Nyltex) to remove any larger parts originating from the sea urchin and diluted to an approximate density of 1000 eggs/ml before fertilization with diluted sperm. When formation of fertilization membranes were observed 1 min after fertilization, 50 μl of the fertilized eggs were transferred to a 96-well plate containing 50 μl of ianthelline solution at different concentrations. Each concentration was tested in parallel and parallels of FSW were used as a control. The number of dividing cells was recorded after 80 min (when 100% of control cells was divided) and 150 min (after the second cell division of the control cells) and 210 min after fertilization. Fertilized eggs were observed with an inverted microscope (×40 magnification). All experiments were performed at 19˚C.

DNA replication in fertilized sea urchin eggs. To avoid hardening of the fertilization membrane, eggs were fertilized in the presence of 1 mM 3-amino-1,2,4-triazole. The fertilization membrane was subsequently removed by filtering the fertilized eggs through a 65-μm nylon filter. The eggs were diluted with FSW to 1000/ml and 900 μl egg suspension, containing 0.3 mg/ml 5-bromo-2-deoxyuridine (BrdU) (Amersham Biosciences Europe GmbH, Freiburg, Germany) and 210 μM ianthelline, was incubated in 24-well plates. Sea urchin embryos exposed to the same DMSO concentration as the ianthelline-exposed sea urchin embryos were used as reference. Eggs were fixed in 4 M HCl for 120 min, post-fixed in MeOH for 30 min and washed twice in AT-buffer [150 mM NaCl, 50 mM Tris-HCl (pH 7.4) and 0.05% Tween-20] before incubation in anti-BrdU mouse monoclonal antibody (Amersham Biosciences Europe GmbH) at 4˚C for 2 h and subsequent rinsing in AT-buffer. Incorporated BrdU was stained with 0.1% fluorescein 5(6)-isothiocyanate (FITC)-conjugated anti-mouse antibody (diluted 1:500 in AT-buffer) for 1 h at 20˚C in darkness. Eggs were washed with AT-buffer and mounted on glass plates in Vectashield (Vector Laboratories, Burlingame, CA, USA). The embryos were examined with a fluorescence microscope at ×60 magnification.

Immunofluorescence staining of microtubules. For immunofluorescence labelling of microtubules, eggs were fertilized and fertilization membranes removed as described above. Fertilized eggs were diluted to 1,000/ml in FSW, and 900 μl of egg suspension, with or without 210 μM ianthelline, were transferred to 4-well plates. Eggs were sampled 40, 90 and 120 min after fertilization and treated with a microtubule-preserving buffer for 60 min. The buffer consisted of 10 mM Na-ethylene glycol tetraacetic acid, 0.55 mM $MgCl_2$, 25 mM 2-(*N*-morpholino)ethanesulfonic acid (MES) (pH 6.8), 25% glycerol and 1% nonylphenyl-polyethylene glycol (NP40). The eggs were fixed for 30 min in 100% MeOH, washed twice in AT-buffer and incubated overnight at 4˚C with anti-tubulin antibody, diluted at 1:100 in AT-buffer. The eggs were then washed twice in AT-buffer, before being incubated with (0.2%) FITC-conjugated anti-mouse antibody diluted, 1:500 in AT-buffer, for 1 hour at 20˚C in darkness. The embryos were then incubated for 1 hour in AT buffer containing 2.5 μg/ml 4',6-diamidino-2-phenylindole (DAPI), washed in AT-buffer, mounted on glass plates in Vectashield and examined with a fluorescence microscope at ×40 magnification.

Kinase inhibition assay. Ianthelline inhibition of the phosphorylation activity of PKA and ABL kinases was measured by incubating them with ianthelline at concentrations of 10.52-210.46 μM in two separate experiments. The extent of kinase inhibition was evaluated using the Kinase Reaction Rate Kit (BioThema, Haninge, Sweden) following the protocol provided by the manufacturer. Inhibition of phosphorylation was measured by monitoring ATP degradation using bioluminesence. Light emission was measured after 5 min and 1 h from the samples in white 384-well microtitre plates (PerkinElmer, Waltham, MA, USA) using an Envision luminescence reader (PerkinElmer). The measured values resulted in data expressed as the percentage kinase inhibition with staurosporine used as positive control.

PTP1B inhibition assay. The enzymatic assay was carried out at 37˚C using the fluorogenic substrate 6,8-difluoro-4-methylumbelliferyl phosphate (DiFMUP; VWR, Leuven, Belgium) and recombinant human PTP1B (Merck-Calbiochem, Darmstadt, Germany). The assay buffer consisted of 25 mM HEPES sodium salt (Alfa Aesar, Karlsruhe, Germany), 50 mM sodium chloride (Merck),

Figure 2. *Frozen specimens of Stryphnus fortis. (Photo: Robert Johansen, Marbank).*

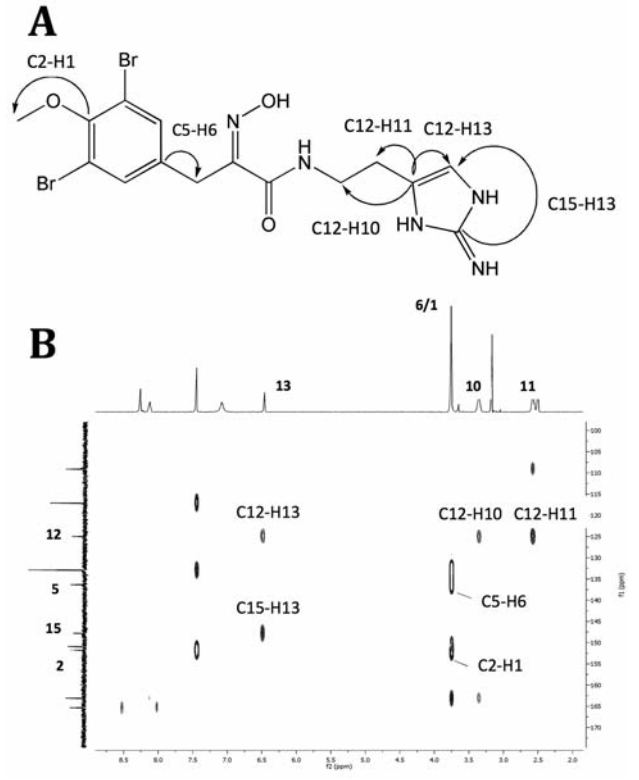

Figure 3. *A: The molecular structure of ianthelline with arrows highlighting ^{1}H-^{13}C heteronuclear multiple bond correlation (HMBC) correlations. B: Magnified HMBC spectrum of ianthelline with correct ^{13}C assignment, illustrating the C-H correlations of the previously mislabelled carbon atoms.*

2 nM 1,4-dithiothreitol (VWR), 2.5 mM ethylene diaminetetra-acetic acid disodium salt dehydrate (Sigma), and 0.01 mg/ml human albumin (Sigma-Aldrich). Ianthelline was diluted in 25 μl of assay buffer to generate test concentrations ranging from 52 to 210 μM and mixed with 50 μl PTP1B dissolved in assay buffer to give 1.56 ng enzyme/well in black 96-well plates. Each concentration was tested

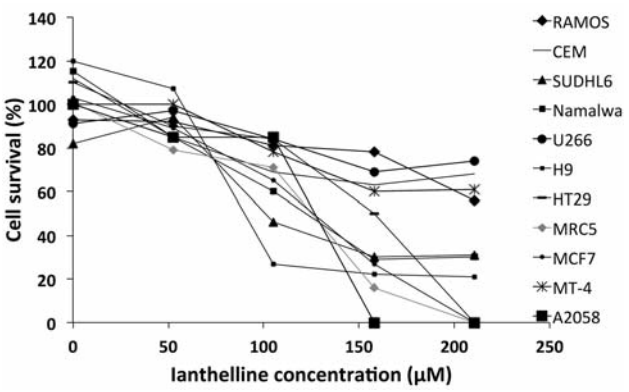

Figure 4. *Cytotoxic evaluation of ianthelline against one non-malignant and ten malignant cell lines after 72 h of ianthelline exposure. Cell proliferation was determined by the MTS assay, and cytotoxicity was found to increase with increasing concentrations of ianthelline. Values are mean of two parallels.*

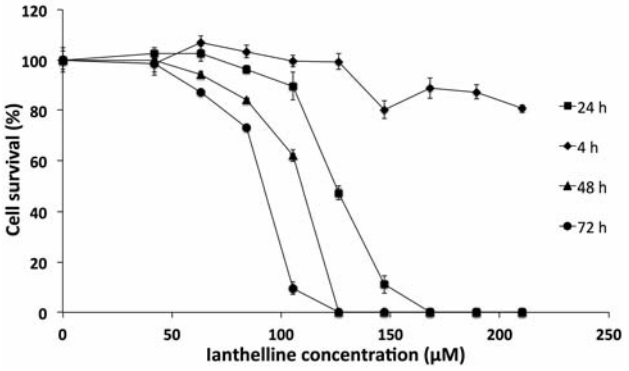

Figure 5. *Dose- and time-dependent effect of ianthelline on A2058 cell proliferation. Cell viability was measured by the MTS assay at the indicated time and concentration. Values are mean of three parallels.*

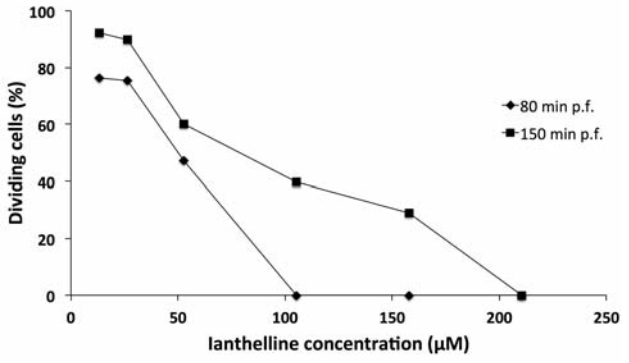

Figure 6. *Dose-response of ianthelline towards Paracentrotus lividus egg division post-fertilization (p.f.). The values are percentages of dividing eggs recorded at 80 and 150 min p.f. and are the mean of two parallels. Controls were incubated in filtered seawater containing the same amount of dimethyl sulfoxide as the treated samples.*

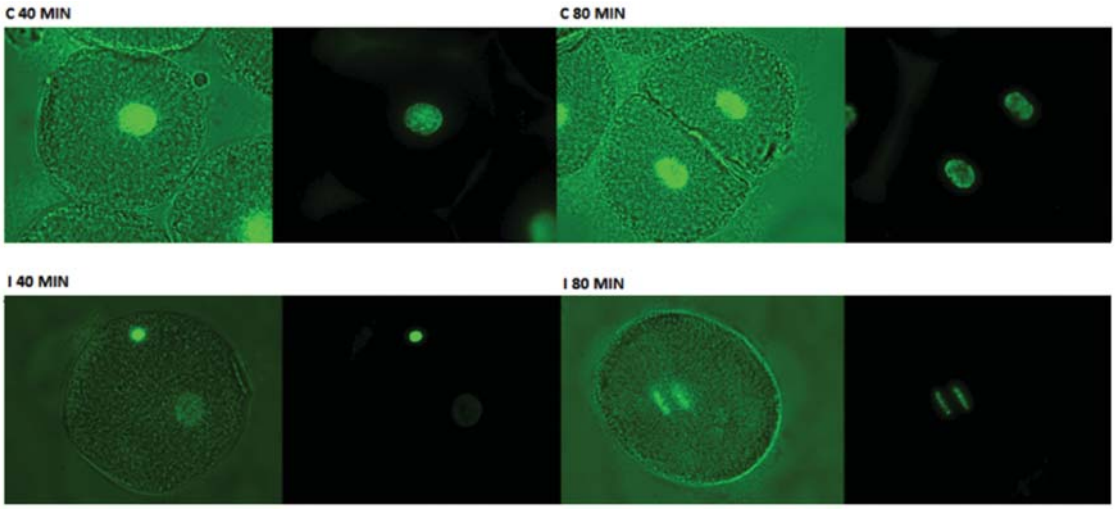

Figure 7. *Monitoring of DNA replication by chromatin incorporation of BrdU in ianthelline-exposed (I) and control (C) fertilized sea urchin embryos. Fertilized eggs were incubated in presence of BrdU, and incorporation was visualised with anti-BrdU antibody followed by staining with fluorescein 5(6)-isothiocyanate (FITC)-conjugated anti-mouse antibody. Control (filtered seawater) and ianthelline (210 μM)-treated embryos were fixed 40 and 80 min post-fertilization (p.f.). In control embryos, DNA synthesis and cell division had occurred 80 min p.f. Ianthelline-exposed embryos had replicated their DNA, but no sign of cytokinesis was evident 80 min p.f. The embryos were examined with a fluorescence microscope at ×60 magnification.*

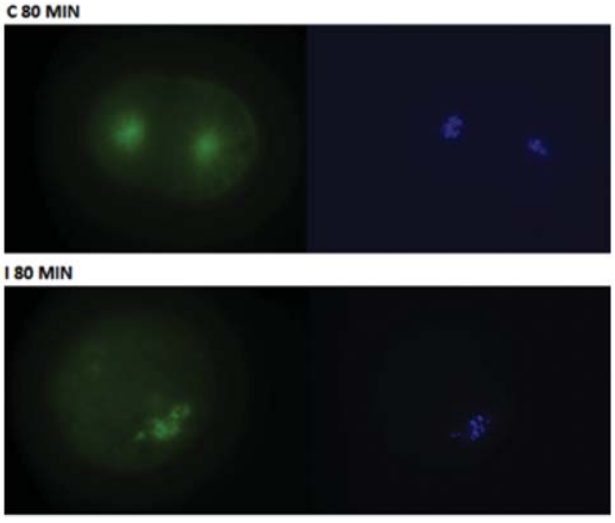

Figure 8. *Monitoring of microtubule assembly in sea urchin embryos by immunofluorescence staining the microtubule with α-tubulin antibodies. Embryos were incubated with mouse anti-α-tubulin antibody and stained with fluorescein 5(6)-isothiocyanate (FITC)-conjugated anti-mouse antibody and 4',6-diamidino-2-phenylindole (DAPI). The green labelling shows the microtubules and the blue staining is of the DNA. Embryos (I) were incubated with 210 μM ianthelline. Control embryos (C) were incubated in filtered seawater without ianthelline; both were fixed 80 min post-fertilization. The embryos were examined with a fluorescence microscope at ×40 magnification.*

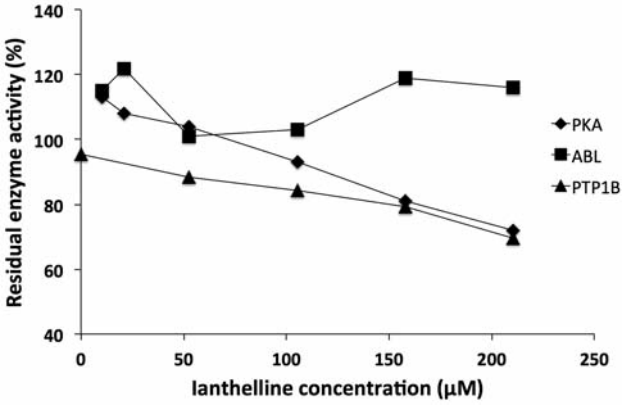

Figure 9. *The effect of ianthelline on the enzymatic activity of cAMP-dependent protein kinase A (PKA), tyrosine kinase ABL (ABL) and protein-tyrosine phosphatase 1B (PTP1B). Enzyme activity was monitored in two separate experiments under standard conditions, as described in the Materials and Methods. Results are expressed as % of control activity in the absence of ianthelline. Each point represents the average of two parallel means.*

in triplicate. After 30-min incubation in the dark, 25 μl 10 μM DiFMUP solution were added and the fluorescent signal was measured with a DTX 880 Multimode Detector (Beckman Coulter) at excitation and emission wavelengths of 360 nm and 465 nm, after 10 min incubation in the dark. The positive control was a 0.16 mM solution of PTP inhibitor IV (Merck-Calbiochem). Assay buffer was used as the negative control. The fluorescent signal was converted to percentage of inhibition by comparing the measured values to those of the positive and negative controls.

Kinase selectivity studies. The ability of ianthelline to selectively inhibit kinases was tested by exposing a panel of 131 kinases to the compound at a concentration of 105.23 μM. The assays were carried

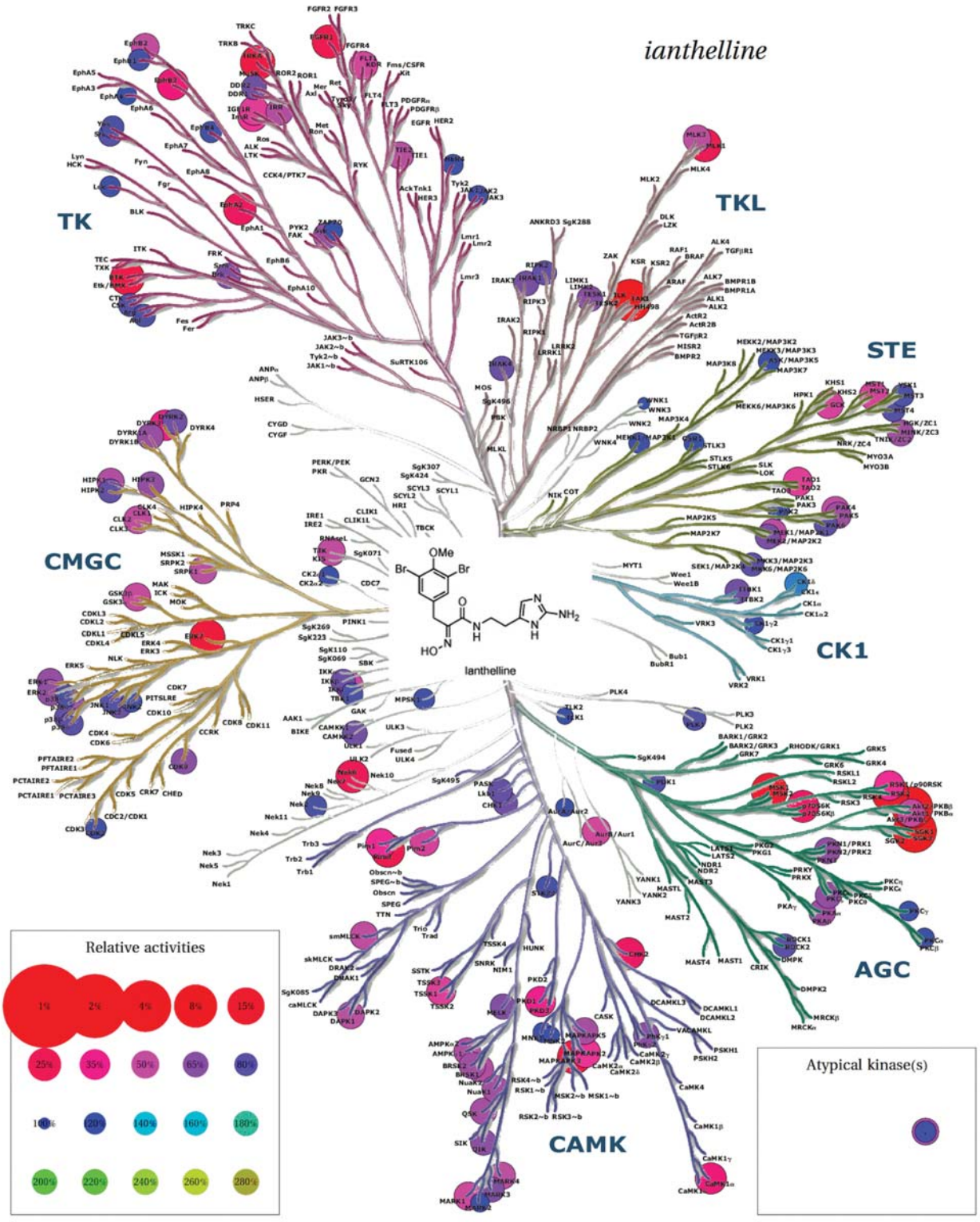

Figure 10. *Kinome inhibition data for ianthelline, with the disc sizes and colours encoding the level of residual activity as shown in the Figure key. With a Gini co-efficient of 0.22 (based on residual activity values), ianthelline is only moderately selective, but shows no obvious preference for any kinase subfamily; it may be valuable as a scaffold for further optimization. At around 10% residual activity, the strongest inhibition is observed for the closely-related kinases AKT2 (PKBb) and serine/threonine-protein kinase SGK1 (SGK1), and for transforming growth factor beta activated kinase 1 (TAK1). The apparent selectivity for AKT2 inhibition compared to AKT1 (PKBa) is remarkable, considering the great similarity of the two enzymes.*

out using a radioactive (^{33}P-ATP) filter-binding assay at the International Centre for Kinase Profiling at the University of Dundee, UK (http://www.kinase-screen.mrc.ac.uk/).

Results

Purification and structure determination. Separation conditions, including sample preparation, injection volumes, and gradient conditions were optimised to successfully separate ianthelline from other compounds in the extract. Ianthelline is the main component in the organic extract from *S. fortis* and 73 collected mass-triggered fractions yielded 45.3 mg from approximately 1 kg of sponge material. Full scan HR-MS analysis showed only negligible amounts of impurities in the isolated compound. The protonated compound gave an *m/z* of 473.9740, corresponding to an elemental composition of $C_{15}H_{17}N_5O_3Br_2$ (calculated *m/z*=473.9776), which matches the elemental composition of ianthelline. The structure of ianthelline initially proposed by Litaudon and Guyot (15) was confirmed by the ^{1}H- and ^{13}C-NMR data. In addition, 2-D experiments, H-H-COSY, HSQC and HMBC, were also performed. The COSY and HSQC yielded the expected data, while the HMBC data yielded correlations that did not match the original published assignment (Table I). In the article from 1986, the carbon signals for the iminoimidazole ring were assigned based on literature values and the C12 signal was assigned given a shift value of 137.2 ppm. Subsequently the signal at 126.0 ppm was assigned to the C5 atom. HMBC analysis of these two carbon signals clearly shows that those two assignments are exchanged. The signal at 126.0 has unambiguous correlations with protons H13, H11 and H10, while the signal at 137.2 only has a correlation with proton H6. Furthermore, the C2 and C15 signals at 148.8 and 153.8 are also erroneous. The C15 atom displays a clear correlation with H13. A cross peak between C2 and the methoxy protons (H1) is also present (Figure 3 A and B). To conclude, the accurate assignment of the four wrongly labelled carbon atoms is as follows, based on HMBC experiments: C5: 137.2 ppm, C2: 126.0 ppm, C2: 153.8 ppm, C15: 148.8 ppm.

Cytotoxic effect on cell lines. The sensitivity of 11 cell lines towards ianthelline was tested and cell survival of non-malignant lung fibroblasts MRC5 and ten different malignant cell lines are shown in Figure 4. All different cell types revealed dose-dependent cytotoxicity. No selectivity between malignant and non-malignant cell lines was apparent. The cytotoxic effect of the compound was further evaluated in the human melanoma cell line A2058 treated with different concentrations of ianthelline for 4, 24, 48, and 72 h (Figure 5). The calculated half maximal inhibitory concentration (IC_{50}) value was found to decrease with increasing exposure time (4 h: no apparent activity, 24 h: 125.2 μM, 48 h: 107.8 μM, 72 h: 91.57 μM), revealing the cytotoxic effect to be both dose- and time-dependent. Trypan blue staining of cells treated with ianthelline for 72 h revealed no loss of cell membrane integrity (data not shown).

Effect of ianthelline on cell-cycle progression in sea urchin embryos. In normal, untreated *P. lividus* embryos, the cytokinesis of the first mitotic division of the cells takes place 70 min after fertilization followed by the second and the third division occurring after 130 and 180 min, respectively. Ianthelline blocked the cell divisions of *P. lividus* embryos in a dose-dependent manner. The cell divisions were severely delayed at an ianthelline concentration of 105 μM, whereas no effect was observed at a concentration of 26 μM (Figure 6). In the control treatments, the number of normally developing embryos ranged between 85 and 90%. By using nonlinear least square model estimation, the IC_{50} value of ianthelline was calculated to be 53 μM. No cell division was observed above 200 μM, even after long-term examination. To examine if the presence of the fertilization membrane had any influence on ianthelline toxicity, it was removed before ianthelline addition. The sensitivity of the sea urchin embryos towards ianthelline was not affected by the removal of the fertilization membrane (data not shown).

Inhibition of DNA synthesis in sea urchin embryos. To evaluate whether ianthelline affects DNA synthesis, DNA replication was monitored by incubating the fertilized eggs in the presence of ianthelline and the nucleotide analogue BrdU, followed by staining with fluorescently-labelled anti-BrdU antibodies. BrdU was incorporated in the chromatin of the normally developing embryos in the control treatment (Figure 7), as well as in the non-dividing eggs treated with ianthelline after 80 min (Figure 7), indicating that DNA replication was not blocked by ianthelline. In newly fertilized eggs, the sperm and egg pronuclei migrate to the centre of the egg and fuse. Concomitantly, DNA replication is observed in the re-formed zygotic nucleus. However, as previously demonstrated (19), DNA synthesis is not dependent on pronuclear fusion. BrdU incorporation in eggs treated with ianthelline was observed in some eggs while the two pronuclei were still separated (Figure 7). This indicates that ianthelline delays pronuclear migration and suggests that the microtubule assembly could be perturbed.

Effect of ianthelline on microtubule organisation and cytokinesis. To monitor microtubule organisation during the first mitotic cell division, the microtubules in fertilized eggs were stained with α-tubulin antibodies. At 80 min post-fertilization, the normally developing embryos in the control treatment had undergone the first cell division and microtubule asters were visualised on top of the nuclei of the two daughter

Table I. *Nuclear magnetic resonance (NMR) assignment of ianthelline compared with the initial assignment of Litaudon and Guyot (1).*

Atom no.	δ_H Purified ianthelline (CD_3OD)	δ_H DMSO (1)	δ_C Purified ianthelline	δ_C CD_3OD (1)	HMBC ^1H-^{13}C	^1H-^1H-COSY
1	3.75 (s)	3.75	60.39	61.00		
2			147.78	148.60		
3/3'			117.10	118.50		
4/4'	7.44 (s)	7.44	132.88	134.40	2, 5, 6	
5			136.32	126.00		
6	3.75 (s)	3.75	27.89	28.80		
7			150.90	152.10		
8			163.09	165.60		
9	8.12 (t)	8.09				10
10	3.36 (q)	3.36	37.52	38.90	8, 11, 12	9, 11
11	2.57 (t)	2.58	24.76	25.70	10, 12, 13	10
12			124.97	137.20		
13	6.46 (s)	6.50	109.12	110.70	12, 15	
14/14'/14"	7.08 (s)	7.37				
15			151.74	153.80		

1 Litaudon M and Guyot M: Ianthelline, un nouveau derive de lfl dibromo-3,5 tyrosine, isole de l'eponge *ianthella ardis* (Bahamas). Tetrahedron Lett *27(37)*: 4455-4456, 1986.

cells (Figure 8). Eggs incubated with ianthelline yielded nucleation of multiple and erratic spindle asters formed around the condensed chromosomes (Figure 8). No cytokinesis occurred, even though chromosome splitting could be seen.

PKA, ABL, and PTP1B inhibition. Ianthelline was tested for inhibition of the activity of PKA and ABL, and was found not to strongly inhibit the phosphorylation of the two protein kinases (Figure 9). However, while weak dose-dependent inhibition of PKA activity was observed, the highest concentration only inhibited 30% of the measured activity. Ianthelline was found to inhibit PTP1B in a similarly weak, but dose-dependent manner (Figure 9).

Kinase selectivity studies. Ianthelline was tested against a panel of 131 kinases in the protein kinase selectivity-screening panel. One kinase, serine/threonine-protein kinase SGK1 (SGK1), had a residual activity of less than 10%, and four kinases, PKBb, ribosomal s6 kinase 2 (RSK2), mitogen- and stress-activated protein kinase 1 (MSK1), and transforming growth factor beta activated kinase 1 (TAK1), had a residual activity of less than 20%. Based on the residual activity levels of all kinases tested, the Gini co-efficient was calculated to be 0.22. Kinome inhibition data for ianthelline can be seen in Figure 10, with the disc size indicating residual kinase activity.

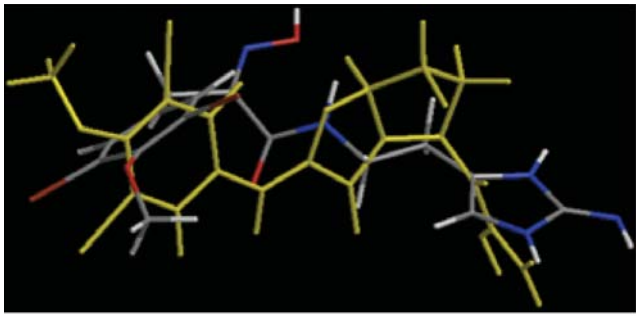

Figure 11. *Molecular similarity three-dimensional alignment of ianthelline and synoxazolidinone C. Ianthelline, normally colour-coded, overlaid with synoxazolidinone C, yellow colour-coded.*

Discussion

Marine species have proven to be a rich source of bioactive secondary metabolites. Success is especially evident for the development of anticancer drugs, with four out of seven FDA-approved marine-derived compounds being anticancer agents. In our study, the previously unknown mode of action of the dibromotyrosine derivative ianthelline was investigated, revealing the potential of ianthelline as an anticancer drug.

Ianthelline was isolated from the Arctic marine sponge *S. fortis*. HR-MS and NMR analyses confirmed the purity and molecular structure of ianthelline. Moreover, NMR analysis clarified a previous misinterpretation of ^{13}C-NMR shift values of ianthelline (see Table I) (15). While the molecular structure of ianthelline is uncontroversial, there has been some ambiguity regarding the assignment of the ^{13}C signals. Based on standard ^{13}C-NMR data analysis, Thirionet *et al*. (20) and Litaudon and Guyot (15) provided alternative assignments. The ambiguity was resolved in the present study by employing heteronuclear correlation experiments. This assignment is in

agreement with the one suggested by Thirionet *et al*. and it is now supported by an accurate spectral explanation.

Ianthelline inhibited the growth of all cancer cell lines tested. The non-malignant cell line MRC5 was also affected, suggesting that ianthelline affects a property common to all cell lines, and not one limited to cancer cells alone. Furthermore, the cytotoxicity of ianthelline against the human melanoma cell line A2058 was found to correlate with increasing exposure time. While no apparent activity was visible after 4 h of exposure, the cell line was increasingly affected after 24-, 48-, and 72-h exposures. This observation suggests that ianthelline interferes with an ongoing cellular process rather than causing cell death by cell membrane lysis. This assumption was further supported by the result of the trypan blue staining which revealed no loss of cell membrane integrity in cells treated with ianthelline for 72 h.

This report gives further insight into the potential cellular mechanisms underlying the toxic effects of ianthelline. A sensitive bioassay based on the first cleavage stages of fertilized sea urchin eggs was used to further investigate the cellular mechanisms generating the ianthelline cell toxicity. The synchronous division of these cells, for which cell-cycle events are easily monitored, allowed the potential anti-proliferative activity of this compound to be addressed. Ianthelline perturbed cell division of sea urchin embryos in a dose-dependent manner from concentrations from 26 μM to 105 μM, where cell division was severely delayed. To evaluate if ianthelline interfered with DNA synthesis, which would lead to disturbance of cytogenesis of these cells (21), the incorporation of BrdU into newly synthesized DNA was monitored. As visualised in Figure 7, DNA synthesis proceeded normally even if the migration and fusion of male and female pronuclei was affected. Like mitotic spindle formation and cytokinesis, male pronucleic migration relies on correct assembly of microtubule arrays. The mitotic spindle is responsible for separating the chromosomes to each side of the cell prior to cytokinesis. Mitotic spindle formation is a dynamic process of polymerisation and de-polymerisation of α- and β-tubulin subunits, and many natural products with anticancer activity target this process (22). To investigate the potential action of ianthelline on microtubule dynamics, tubulin was stained in sea urchin embryos. It became apparent from the results that ianthelline disturbed the assembly of the mitotic spindle in sea urchin embryos treated with 210 μM ianthelline (Figure 8). The microtubules were arranged erratically, and no cell division occurred in the cells treated with ianthelline, indicating that microtubule assembly is an intra cellular process targeted by this compound.

Furthermore, the cytotoxic effect of ianthelline was found to possibly involve kinase inhibition. Ianthelline was tested for inhibitory activity against PTP1B and the kinases PKA and ABL in a reaction rate assay, and kinase inhibition profiling was carried out at the University of Dundee. In Dundee, 131 kinases were exposed to an ianthelline concentration of 105 μM. Although the Dundee panel shows only weak inhibition of PKA for ianthelline, the closely related kinases AKT2 (PKBb) and SGK1 are among the most strongly inhibited protein kinases; a third is the TKL kinase TAK1. Notable here is the observation of the selectivity of ianthelline for AKT2 over AKT1, as the two kinases are nearly identical at the ATP-binding site, and both closely resemble PKA (23). The Gini co-efficient for the degree of selectivity of ianthelline is calculated to be 0.22, which would indicate ianthelline to be more selective than *e.g*. staurosporine (0.09), but quite far from the value of 0.80 for the highly selective inhibitor PD184352 (24). This has little bearing on the potential value of ianthelline as a scaffold for protein kinase inhibition, however, because the necessary optimisation of inhibitory potency would also substantially alter the selectivity profile.

Compounds displaying general cytotoxicity have previously been isolated from marine sponges (25), including fascaplysin (26), laulimalide (27), and spongistatin 1 (28). A chemical defence is unquestionably among the most important defence strategies of sponges (29), and several of these are produced to act as general toxins to repel predators or to hinder biofouling on its surface (30). Each sponge produces a characteristic mixture of metabolites, some exclusive to its species and some with wider distribution. The secondary metabolite ianthelline has previously been isolated from the Bahamian sponge *Ianthella ardis* (15), and here it was found in the Arctic sponge *S. fortis*. Finding a common secondary metabolite in sponges belonging to different orders is uncommon, but it occasionally happens, with the antitumor and antibacterial compound discohabin D being another example (31). Even though conditions vary greatly between the Bahamas and the Arctic, the threats from their biotic environment are comparable, which would explain the presence of ianthelline in two seemingly unrelated sponges. To our knowledge, no other bioactive compounds have been isolated from the species *S. fortis* or from the *Stryphnus* genus.

Unlike terrestrial organisms, marine organisms often produce halogenated secondary metabolites, with bromoalkaloids being the most widely distributed, many originating from sponges (32). In addition to ianthelline, several other bromotyrosine derivatives have been isolated from marine sponges (33), examples of which are purealin (34) and ianthesines A-D (35).

In this study, the cytotoxic properties of ianthelline, a dibromotyrosine derivative isolated from the Arctic sponge *S. fortis* was evaluated. The molecular structure of ianthelline was confirmed by HR-MS and NMR analysis. Ianthelline was found to reduce cell viability, inhibit sea urchin embryo cell division, disturb mitotic spindle assembly, and to inhibit kinase activity with a Gini co-efficient of 0.22. Cell death was found not to be due to cell membrane lysis, as cell membrane of cell lines treated with ianthelline for 72 h were

still intact. Nor was cell death found to be due to inhibition of DNA synthesis. We have demonstrated that the disruption of microtubule assembly is a likely target for the cytotoxicity activity of ianthelline in addition to the inhibition of a range of protein kinases. Ianthelline represents an interesting scaffold for the production of bioselective derivatives to design ianthelline-related compounds as anticancer agents with higher selectivity towards cancer cells and higher potency than the parent ianthelline molecule. For example, ianthelline shares several similarities with the dibrominated guanidinium 4-oxazolidinones derivative synoxazolidinone C, with promising bioactivities, isolated from the sub-Arctic ascidian *Synoicum pulmonaria* (Figure 11). The focus for future studies involving ianthelline should evolve around elucidation of the structure-activity relationship and chemical synthesis of analogues with improved bioactivities and selectivity to become drug candidates.

Acknowledgements

We would like to thank Marbank for sponge collection, identification and extract preparation. MabCent is a centre at the University of Tromsø and is supported by the Research Council of Norway, Grant no 174885/130. The Authors also acknowledge the support of the European Community-Research Infrastructure Action under the FP7 Specific Programme (ASSEMBLE grant agreement no. 227799).

References

1 Cragg GM, Grothaus PG and Newman DJ: Impact of natural products on developing new anti-cancer agents. Chem Rev *109(7)*: 3012-3043, 2009.

2 Gerwick W and Moore B: Lessons from the past and charting the future of marine natural products drug discovery and chemical biology. Chem Biol *19(1)*: 85-98, 2012.

3 Feher M and Schmidt JM: Property distributions: Differences between drugs, natural products, and molecules from combinatorial chemistry. J Chem Inf Comput Sci *43(1)*: 218-227, 2003.

4 Martín JF, Casqueiro J and Liras P: Secretion systems for secondary metabolites: How producer cells send out messages of intercellular communication. Curr Opin Microbiol *8(3)*: 282-293, 2005.

5 Dixon N, Wong LS, Geerlings TH and Micklefield J: Cellular targets of natural products. Nat Prod Rep *24(6)*: 1288-1310, 2007.

6 Rosen J, Gottfries J, Muresan S, Backlund A and Oprea TI: Novel chemical space exploration via natural products. J Med Chem *52(7)*: 1953-1962, 2009.

7 van Soest RWM: Sponge biodiversity. J Mar Biol Assoc UK *87(06)*: 1345-1348, 2007.

8 Belarbi EH, Contreras Gómez A, Chisti Y, Garcıa Camacho F and Molina Grima E: Producing drugs from marine sponges. Biotechnol Adv *21(7)*: 585-598, 2003.

9 Berrue F, Thomas OP, Laville R, Prado S, Golebiowski J, Fernandez R and Amade P: The marine sponge *Plakortis zyggompha*: A source of original bioactive polyketides. Tetrahedron *63(10)*: 2328-2334, 2007.

10 Schumacher M, Kelkel M, Dicato M and Diederich M: Gold from the sea: Marine compounds as inhibitors of the hallmarks of cancer. Biotechnol Adv *29(5)*: 531-547, 2011.

11 Tadesse M, Gulliksen B, Strom MB, Styrvold OB and Haug T: Screening for antibacterial and antifungal activities in marine benthic invertebrates from northern Norway. J Invertebr Pathol *99(3)*: 286-293, 2008.

12 Yasuhara-Bell J and Lu Y: Marine compounds and their antiviral activities. Antiviral Res *86(3)*: 231-240, 2010.

13 Mayer AM, Rodriguez AD, Berlinck RG and Fusetani N: Marine pharmacology in 2007-8: Marine compounds with antibacterial, anticoagulant, antifungal, anti-inflammatory, antimalarial, antiprotozoal, antituberculosis, and antiviral activities; affecting the immune and nervous system, and other miscellaneous mechanisms of action. Comp Biochem Physiol C Toxicol Pharmacol *153(2)*: 191-222, 2011.

14 Natori T, Morita M, Akimoto K and Koezuka Y: Agelasphins, novel antitumor and immunostimulatory cerebrosides from the marine sponge *Agelas mauritianus*. Tetrahedron *50(9)*: 2771-2784, 1994.

15 Litaudon M and Guyot M: Ianthelline, un nouveau derive de lfl dibromo-3,5 tyrosine, isole de l'eponge *Ianthella ardis* (Bahamas). Tetrahedron Lett *27(37)*: 4455-4456, 1986.

16 Shearman JW, Myers RM, Beale TM, Brenton JD and Ley SV: Total syntheses of the bromotyrosine-derived natural products ianthelline, 5-bromoverongamine and JBIR-44. Tetrahedron Letters *51(37)*: 4812-4814, 2010.

17 Yip SC, Saha S and Chernoff J: PTP1B: a double agent in metabolism and oncogenesis. Trends Biochem Sci *35(8)*: 442-449, 2010.

18 Wood LD, Parsons DW, Jones S, Lin J, Sjoblom T, Leary RJ, Shen D, Boca SM, Barber T, Ptak J, Silliman N, Szabo S, Dezso Z, Ustyanksky V, Nikolskaya T, Nikolsky Y, Karchin R, Wilson PA, Kaminker JS, Zhang Z, Croshaw R, Willis J, Dawson D, Shipitsin M, Willson JK, Sukumar S, Polyak K, Park BH, Pethiyagoda CL, Pant PV, Ballinger DG, Sparks AB, Hartigan J, Smith DR, Suh E, Papadopoulos N, Buckhaults P, Markowitz SD, Parmigiani G, Kinzler KW, Velculescu VE and Vogelstein B: The genomic landscapes of human breast and colorectal cancers. Science *318(5853)*: 1108-1113, 2007.

19 Sluder G, Thompson EA, Rieder CL and Miller FJ: Nuclear envelope breakdown is under nuclear not cytoplasmic control in sea urchin zygotes. J Cell Biol *129(6)*: 1447-1458, 1995.

20 Thirionet I, Daloze D, Braekman JC and Willemsen P: 5-Bromoverongamine, a novel antifouling tyrosine alkaloid from the sponge *Pseudoceratina* sp. Nat Prod Res *12(3)*: 209-214, 1998.

21 Geneviere-Garrigues AM, Barakat A, Doree M, Moreau JL and Picard A: Active cyclin B-cdc2 kinase does not inhibit DNA replication and cannot drive prematurely fertilized sea urchin eggs into mitosis. J Cell Sci *108(Pt 7)*: 2693-2703, 1995.

22 Jordan MA and Wilson L: Microtubules as a target for anticancer drugs. Nat Rev Cancer *4(4)*: 253-265, 2004.

23 Gassel M, Breitenlechner CB, Ruger P, Jucknischke U, Schneider T, Huber R, Bossemeyer D and Engh RA: Mutants of protein kinase A that mimic the ATP-binding site of protein kinase B (AKT). J Mol Biol *329(5)*: 1021-1034, 2003.

24 Graczyk PP: Gini coefficient: a new way to express selectivity of kinase inhibitors against a family of kinases. J Med Chem *50(23)*: 5773-5779, 2007.

25 Sipkema D, Franssen MC, Osinga R, Tramper J and Wijffels RH: Marine sponges as pharmacy. Mar Biotechnol (NY) *7(3)*: 142-162, 2005.
26 Soni R, Muller L, Furet P, Schoepfer J, Stephan C, Zumstein-Mecker S, Fretz H and Chaudhuri B: Inhibition of cyclin-dependent kinase 4 (Cdk4) by fascaplysin, a marine natural product. Biochem Biophys Res Commun *275(3)*: 877-884, 2000.
27 Mooberry SL, Tien G, Hernandez AH, Plubrukarn A and Davidson BS: Laulimalide and isolaulimalide, new paclitaxel-like microtubule-stabilizing agents. Cancer Res *59(3)*: 653-660, 1999.
28 Bai R, Cichacz ZA, Herald CL, Pettit GR and Hamel E: Spongistatin 1, a highly cytotoxic, sponge-derived, marine natural product that inhibits mitosis, microtubule assembly, and the binding of vinblastine to tubulin. Mol Pharmacol *44(4)*: 757-766, 1993.
29 Ruzicka R and Gleason DF: Sponge community structure and anti-predator defenses on temperate reefs of the South Atlantic Bight. J Exp Mar Bio Ecol *380(1-2)*: 36-46, 2009.
30 Hartmann T: From waste products to ecochemicals: Fifty years research of plant secondary metabolism. Phytochemistry *68(22-24)*: 2831-2846, 2007.
31 Perry NB, Blunt JW and Munro MHG: Discorhabdin D, an antitumor alkaloid from the sponges *Latrunculia brevis* and *Prianos* sp. J Org Chem *53(17)*: 4127-4128, 1988.
32 Dembitsky VM: Bromo- and iodo-containing alkaloids from marine microorganisms and sponges. Bioorg Khim *28(3)*: 196-208, 2002.
33 Okamoto Y, Ojika M, Suzuki S, Murakami M and Sakagami Y: Iantherans A and B, unique dimeric polybrominated benzofurans as Na,K-ATPase inhibitors from a marine sponge, *Ianthella sp*. Bioorg Med Chem *9(1)*: 179-183, 2001.
34 Nakamura Y, Kobayashi M, Nakamura H, Wu H, Kobayashi J and Ohizumi Y: Purealin, a novel activator of skeletal muscle actomyosin ATPase and myosin EDTA-ATPase that enhanced the superprecipitation of actomyosin. Eur J Biochem *167(1)*: 1-6, 1987.
35 Okamoto Y, Ojika M, Kato S and Sakagami Y: Ianthesines A–D, four novel dibromotyrosine-derived metabolites from a marine sponge, *Ianthella* sp. Tetrahedron *56(32)*: 5813-5818, 2000.

Received June 22, 2012
Revised July 27, 2012
Accepted July 30, 2012